

# Luminous superclusters: remnants from inflation

J. Einasto<sup>1</sup>, M. Einasto<sup>1</sup>, E. Saar<sup>1</sup>, E. Tago<sup>1</sup>, L. J. Liivamägi<sup>1</sup>, M. Jõeveer<sup>1</sup>, I. Suhhonenko<sup>1</sup>, G. Hütsi<sup>1</sup>, J. Jaaniste<sup>2</sup>, P. Heinämäki<sup>3</sup>, V. Müller<sup>4</sup>, A. Knebe<sup>4</sup>, and D. Tucker<sup>5</sup>

<sup>1</sup> Tartu Observatory, EE-61602 Tõravere, Estonia

<sup>2</sup> Estonian University of Life Sciences

<sup>3</sup> Tuorla Observatory, Väisäläntie 20, Piikkiö, Finland

<sup>4</sup> Astrophysical Institute Potsdam, An der Sternwarte 16, D-14482 Potsdam, Germany

<sup>5</sup> Fermi National Accelerator Laboratory, MS 127, PO Box 500, Batavia, IL 60510, USA

Received 2006; accepted

**Abstract.** We derive the luminosity and multiplicity functions of superclusters compiled for the 2dF Galaxy Redshift Survey, the Sloan Digital Sky Survey (Data Release 4), and for three samples of simulated superclusters. We find for all supercluster samples Density Field (DF) clusters, which represent high-density peaks of the class of Abell clusters, and use median luminosities/masses of richness class 1 DF-clusters to calculate relative luminosity/mass functions. We show that the fraction of very luminous (massive) superclusters in real samples is more than tenfolds greater than in simulated samples. Superclusters are generated by large-scale density perturbations which evolve very slowly. The absence of very luminous superclusters in simulations can be explained either by non-proper treatment of large-scale perturbations, or by some yet unknown processes in the very early Universe.

**Key words.** cosmology: large-scale structure of the Universe – clusters of galaxies; cosmology: large-scale structure of the Universe – Galaxies; clusters: general

## 1. Introduction

Superclusters are the largest density enhancements in the Universe of common origin. Superclusters evolve slowly and contain information from the very early Universe. The investigation of large systems of galaxies was pioneered by the study of the *Local Supercluster* by de Vaucouleurs (1953). Another approach to define superclusters was initiated by Abell (1958, 1961), who considered them as “*clusters of clusters*”. Until recently, superclusters have been found mostly on the basis of catalogues of rich clusters of galaxies by Abell (1958) and Abell et al. (1989). Abell supercluster catalogues have been compiled by Zucca et al. (1993), Einasto et al. (1994, 1997b, 2001) and Kalinkov & Kuneva (1995).

Actually superclusters consist of galaxy systems of different richness: single galaxies, galaxy groups and clusters, aligned to chains (filaments). This has already been realized before by Jõeveer, Einasto & Tago (1978), Gregory & Thompson (1978), Zeldovich, Einasto & Shandarin (1982), and has been confirmed by recent studies of superclusters using new deep galaxy surveys, such as the Las Campanas Galaxy Redshift Survey, the 2 degree Field Galaxy Redshift Survey (2dFGRS, Colless et al. 2001, 2003) and the Sloan Digital Sky Survey Data Release 4 (SDSS DR4, Adelman-McCarthy et al. 2006). New galaxy redshift surveys are almost complete in a fixed ap-

parent magnitude interval. This allows to estimate total luminosities of superclusters using weights, inversely proportional to the number of galaxies in the observational window of apparent magnitudes. This possibility has been used in recent supercluster studies by Basilakos (2003), Basilakos et al. (2001), Erdogdu et al. (2004), Porter and Raychaudhury (2005), and Einasto et al. (2003a, 2003b, 2005, 2006a, hereafter Paper I).

In Paper I we compiled a catalog of superclusters using the 2dFGRS. A similar catalogue on the basis of SDSS Data Release 4 (DR4) is in preparation (Einasto et al. 2006c, hereafter E06c). The properties of 2dFGRS superclusters were analyzed by Einasto et al. (2006b, Paper II). The parameters of 2dFGRS superclusters were compared with properties of model superclusters based on the Millennium Simulation of the evolution of the Universe by Springel et al. (2005). This comparison of real superclusters with simulated ones shows that geometric properties of simulated superclusters agree very well with similar properties of real superclusters. This demonstrates that the ability to simulate processes which lead to the formation of superclusters has reached an advanced stage. However, one property of model superclusters is in conflict with reality: real samples have many more very luminous superclusters than model samples. The presence of very massive superclusters in our neighborhood is well known, examples are the Shapley and Horologium-Reticulum Superclusters (see Fleener et al. 2005, Proust et al. 2006, Nichol et al. 2006 and Ragone et al. 2006 and

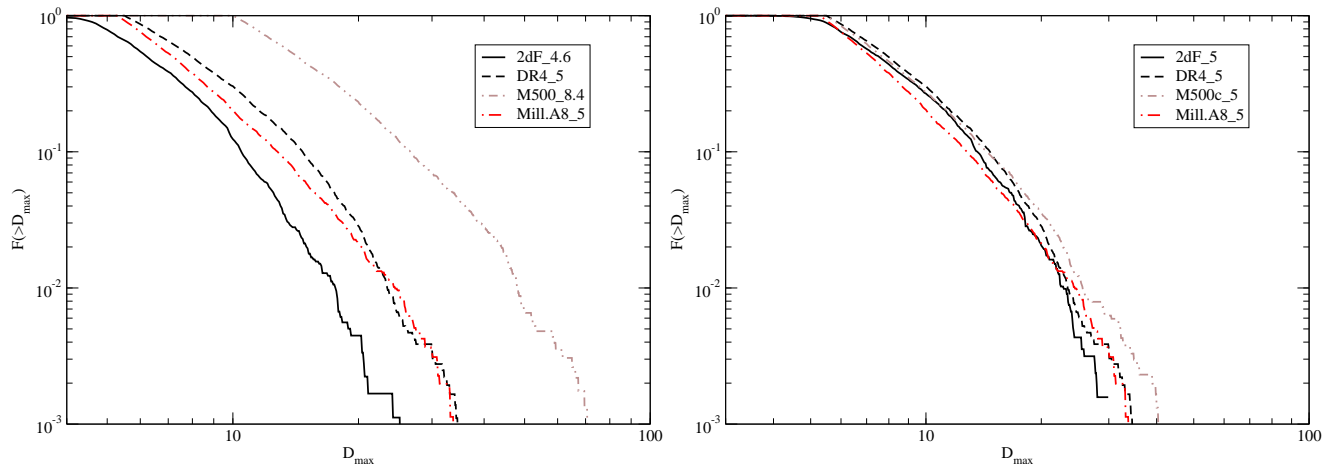


**Fig. 1.** The cumulative distribution of peak densities of DF-clusters. Left panel shows densities uncorrected for the relative bias, right panel densities corrected for differences in the relative bias.

references therein). However, the number of such extremely massive superclusters was too small to make definite conclusions on the phenomenon.

The goal of this Letter is to determine the luminosity and multiplicity functions of 2dFGRS and SDSS DR4 superclusters and to compare these functions with similar functions of simulated superclusters. These observational samples of superclusters are the largest available today. To verify the robustness of the results obtained with the Millennium simulation data we also use superclusters derived from a cosmological simulation of the same volume but with a lower mass resolution. This large collection of real and model superclusters allows us to make definite conclusions on the statistics of luminous superclusters. Supercluster catalogues of the 2dFGRS, as well as fits files of luminosity density fields of 2dFGRS and Millennium Simulation are available electronically at the website <http://www.aai.ee/~maret/2dfsc1.html>.

## 2. Data

In this analysis we used galaxy and group samples of the 2dFGRS (Tago et al. 2006a, Paper I) and SDSS DR4 (Tago et al. 2006b, E06c), and three simulated samples. To compile supercluster catalogues we used the density field method which allows to correct the field to take into account the presence of faint galaxies outside the observational window, for details see Paper I. The richness of a supercluster can be characterised by its total luminosity, and by the number of rich galaxy clusters in it, i.e. the multiplicity function of the supercluster. In Papers I and II we derived both these characteristics. The sample of Abell clusters covers only our close neighbourhood, in more distant superclusters they are found only in exceptional cases. To have a richness parameter we used instead of Abell clusters high-density peaks of the density field, which we call DF-clusters. The spatial density of DF-clusters is approximately close to the spatial density of Abell clusters, thus their utilization as richness indicator yields results comparable with previous supercluster studies based on Abell clusters.

For comparison to the observational data sets we used the galaxy catalogues based upon the Millennium Simulation, for details see Springel et al. (2005), Gao et al. (2005) and Croton et al. (2006). In addition, we also performed a cosmological dark matter simulation of a computational volume of side-length  $500 h^{-1}$  Mpc using  $256^3$  particles (model M500). We chose the concordance cosmology with the parameters  $\Omega_m = 0.27$ ,  $\Omega_\Lambda = 0.73$ ,  $\sigma_8 = 0.84$ . The simulation was carried out with the open source Multi Level Adaptive Particle Mesh (MLAPM) code by Knebe et al. (2001) and DM-halos have been found by the conventional Friends-of-Friends (FoF) procedure. We denote simulated samples as Mill.A8 and M500. The density fields of these models were calculated using all simulation galaxies/particles. In addition, we used the model Mill.F8, where galaxies were chosen using similar selection criteria as in the 2dFGRS sample (see Paper I).

To get comparable results for the luminosity and multiplicity functions of different samples all data and data reduction procedures must be as similar as possible. First of all, density fields must have identical threshold bias levels. We use in our study relative densities expressed in units of the mean density of the particular sample. To check the relative bias levels we found for all samples the threshold density, which yields non-percolating superclusters of maximal diameter approximately  $100 - 120 h^{-1}$  Mpc, and selected DF-clusters using a threshold density about 10 % higher than used in the selection of superclusters.

The comparison of peak densities of DF-clusters in differing samples used in the present study shows considerable disparities amongst the samples, see Fig. 1. These variations are due to differences in mean densities used in the calculation of relative densities, i.e. differences in the threshold bias factor (for a detailed discussion of this phenomenon see Einasto et al. 1999). Fig. 1 shows that peak density distributions of DF-clusters of the SDSS and Millennium simulation samples are practically identical, thus we have used these samples as a standard. To bring the threshold biases of the other samples to a comparative level we divided the density fields of the 2dFGRS samples by 0.739, and the model M500 density field by 2.025

**Table 1.** Data on supercluster samples

| Sample  | $V$   | $N_{gal}$ | $D_0 = 5.0$ |           |       |          |          |           | $D_0 = 6.0$ |           |       |          |          |           |
|---------|-------|-----------|-------------|-----------|-------|----------|----------|-----------|-------------|-----------|-------|----------|----------|-----------|
|         |       |           | $N_{cl}$    | $N_{scl}$ | $N_1$ | $L_0$    | $n_{cl}$ | $n_{scl}$ | $N_{cl}$    | $N_{scl}$ | $N_1$ | $L_0$    | $n_{cl}$ | $n_{scl}$ |
| 2dFz    | 30.3  | 184395    | 2555        | 567       | 279   | 6.86e+11 | 84       | 19        | 1664        | 544       | 265   | 8.20e+11 | 55       | 18        |
| SDSS    | 43.9  | 368002    | 3621        | 1012      | 517   | 7.09e+11 | 82       | 23        | 2364        | 911       | 483   | 8.11e+11 | 54       | 21        |
| Mill.A8 | 125.0 | 8964936   | 4914        | 2259      | 1292  | 1.64e+12 | 39       | 18        | 2878        | 1733      | 1025  | 2.10e+12 | 23       | 14        |
| Mill.F8 | 125.0 | 2094187   | 3020        | 1299      | 762   | 3.08e+12 | 24       | 10        | 1687        | 1068      | 752   | 3.03e+12 | 14       | 8         |
| M500c   | 125.0 | 9785827   | 3032        | 1860      | 1281  | 4.75e+14 | 24       | 15        | 1880        | 1440      | 1037  | 5.81e+14 | 15       | 12        |

(these values were found by comparing peak density distributions shown in the left panel of Fig. 1). The distribution of peak densities of the corrected density fields is shown in the right panel of Fig. 1. We see that there are practically no systematic differences between various samples. These corrected density fields were used to compile the supercluster catalogues used throughout this study.

To obtain comparable results we used for all samples identical procedures in the preparation of the data. In all cases superclusters were found using a luminosity (or mass) density field smoothed with an Epanechnikov kernel of radius  $8 h^{-1}$  Mpc. For observational samples densities were calculated using weights of galaxies which take into account galaxies and galaxy groups too faint to fall into the observational window of absolute magnitudes at the distance of the galaxy. This is the conventional approach for obtaining the luminosity density field (Basilakos et al. 2001, Paper I). The density field was found for a cell size of  $1 h^{-1}$  Mpc, which allows to investigate in detail the internal structure of superclusters (see Paper II). Superclusters were defined as connected non-percolating systems with densities above a certain threshold density. This threshold density is similar to the linking length used in the Friends-of-Friends (FoF) method to find systems of galaxies (or particles in simulations).

Supercluster catalogues have been compiled for two values of the threshold density, i.e.  $D_0 = 5.0$  and  $6.0$  (in units of the corrected mean density). In both cases a lower limit of the supercluster volume of  $100 (h^{-1} \text{ Mpc})^3$  was applied. The main characteristics of these catalogues have been summarized in Table 1: the name of the sample (c indicates the use of corrected density fields as described above),  $V$  is the volume (in million cubic  $h^{-1}$  Mpc),  $N_{gal}$  is the number of galaxies (or particles in case of the model M500c) used in the determination of the density field and the luminosity/mass of superclusters. Next we give for both threshold densities the number of DF-clusters in the sample,  $N_{cl}$  (to derive DF-clusters we used threshold densities 5.5 and 6.5 for the supercluster samples 5.0 and 6.0, respectively).  $N_{scl}$  and  $N_1$  are the total number of superclusters, and the number of superclusters of multiplicity 1 (i.e. containing just one DF-cluster), respectively.  $L_0$  is the mean luminosity (or mass for M500c) of superclusters of multiplicity 1, expressed in Solar units. These luminosities/masses were used in the calibration of relative luminosity functions, see the next section for details. Finally,  $n_{cl}$  and  $n_{scl}$  are the mean spatial densities of DF-clusters and superclusters: the number of objects

per million cubic  $h^{-1}$  Mpc. The threshold density 6.0 for the corrected density field of the 2dFGRS sample corresponds to a threshold density of 4.4 in the uncorrected density field, very close to the value 4.6 used in Paper I to find 2dFGRS superclusters. Thus the number of superclusters and their parameters is very close to the respective data used in Paper I.

### 3. The luminosity and multiplicity functions of superclusters

We shall use in this paper two independent parameters to characterise quantitatively the richness of a superclusters: the multiplicity and the total luminosity (or mass). We define the multiplicity of a supercluster by the number of DF-clusters in it. DF-clusters are high-density peaks of the density field, smoothed on a scale of  $8 h^{-1}$  Mpc. As seen from Table 1, for threshold density  $D_0 = 6.0$  the spatial density of DF-clusters in our samples is about twice the spatial density of Abell clusters, 25 per million cubic  $h^{-1}$  Mpc (Einasto et al. 1997b); for a threshold density of 5.0 the density is somewhat higher. The other integral parameter of a supercluster is its total luminosity or mass, determined by summing luminosities/masses of all galaxies and groups of galaxies (DM-particles) inside the threshold iso-density contour which was used in the definition of superclusters. The relationship between the multiplicity and total luminosity (or mass for M500) is presented in Fig. 2. We see that luminosities have a rather large spread for superclusters of given multiplicity, the lower the multiplicity the larger the spread. The other feature, seen in Fig. 2, is the shift in the mean luminosities of superclusters for different samples. Partly this may be caused by the use of different color systems in various samples.

We are interested in the relative fraction of rich and very rich superclusters in respect to the number of poor superclusters. To avoid complications due to the use of different color systems and masses in case of the model M500, we define *relative* luminosities (masses) as the luminosity (mass) in terms of the mean luminosity (mass) of poor superclusters, i.e. superclusters that only contain one DF-cluster and hence are classified as richness class 1. The distribution of luminosities is approximately symmetrical on a logarithmic scale (see Fig. 2). We therefore used the logarithm of the luminosity to derive the mean value. This value,  $L_0$ , is also listed for all samples in Table 1, in units of the Solar luminosity (mass).

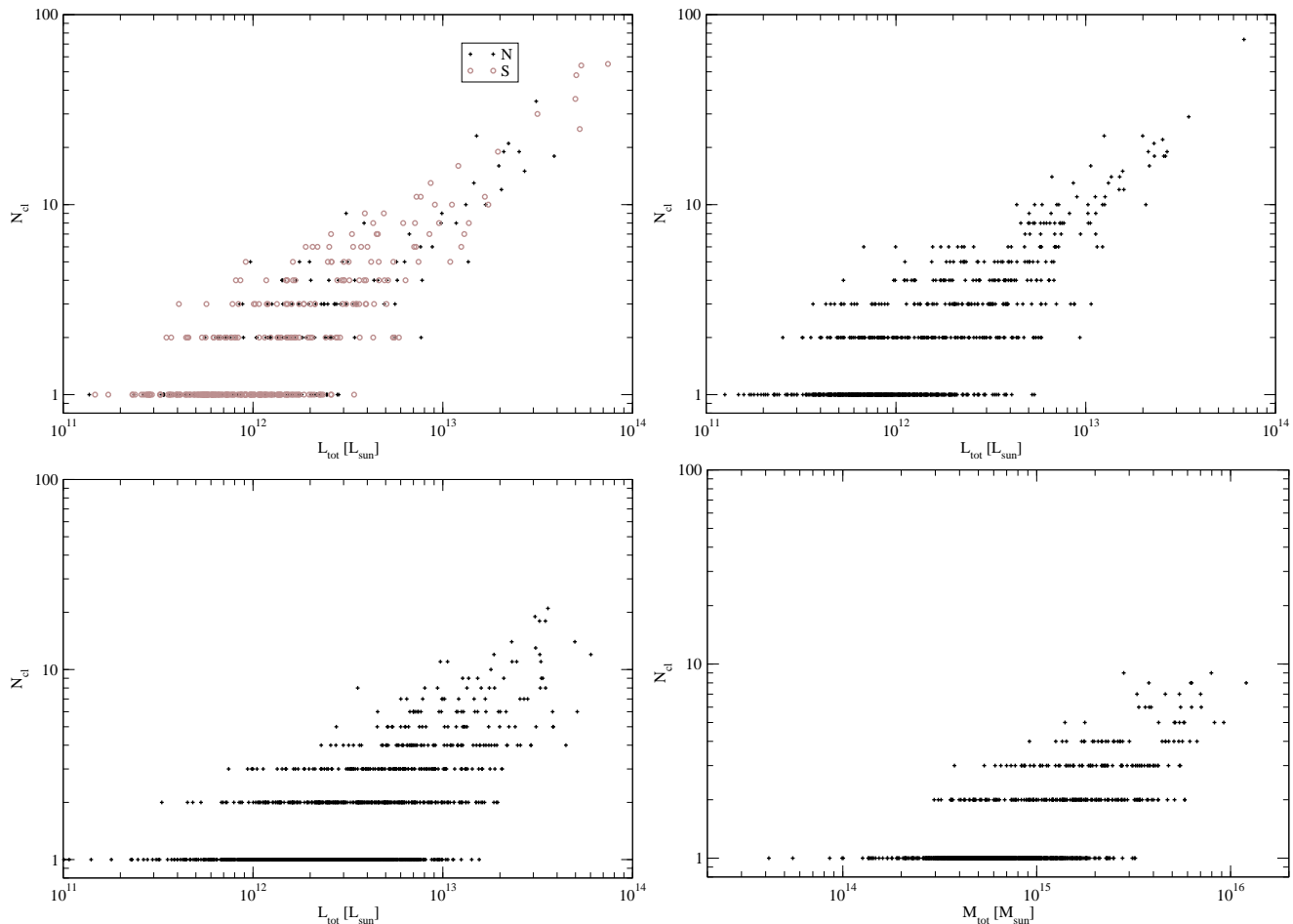


**Fig. 2.** The relationship between the multiplicity and the total luminosity (mass) of real and simulated superclusters, calculated for threshold density 6.0. The samples are: 2dFGRS (top left), SDSS DR4 (top right), Millennium Simulation Mill.A8 (bottom left), the DM simulation M500 (bottom right).

In Fig. 3 we now show the relative luminosity (mass) functions (left panels) alongside the multiplicity functions (right panels) for the observational and model samples. The spatial density of superclusters is expressed in terms of the total number of superclusters in the respective sample to avoid small differences due to the mean number density of superclusters in different samples. In upper panels these functions are shown for all observational and model samples using threshold density 5.0, in lower panels only for the combined observational samples Obs1 and Obs2 (see below), and model samples Mill.A8 and Mill.F8, using threshold density 6.0. The comparison of data obtained with threshold densities 5.0 and 6.0 shows that in the first case some superclusters of the real sample are actually percolating (the maximal diameter of the largest superclusters is almost  $200 h^{-1}$  Mpc). For this reason we have used in the final analysis supercluster samples found with threshold density 6.0.

Upper panels of Fig. 3 show that there are small differences between the observational samples 2dFGRS and SDSS: the 2dFGRS sample contains relatively more rich and very rich superclusters. These differences may be due to the differing depth of these samples: the limiting magnitude of the 2dFGRS sample is about 19.35, whereas that of the SDSS sam-

ple is 17.7. Clusters form superclusters via intermediate density galaxy bridges. The 2dFGRS sample contains more faint galaxy bridges between high-density regions which facilitates the formation of more luminous superclusters. A similar difference is observed between the two model samples. The Mill.A8 sample has a very high spatial resolution and contains numerous faint galaxies which also acts in favour of joining nearby high-density regions via galaxy bridges.

To check this explanation of the difference between samples of various depth we used the simulated 2dFGRS sample Mill.F8, containing only galaxies brighter than 19.35, and calculated for this sample luminosity and multiplicity functions as for other superclusters samples, using threshold densities 5.0 and 6.0. These versions are also shown in Fig. 3. We see that in this case the fraction of luminous superclusters is lower than for the full sample Mill.A8. This test shows that faint galaxy bridges between clusters play indeed an important role in the formation of superclusters. To reduce the SDSS DR4 supercluster sample to the same level of bridge strength as the 2dFGRS sample, a lower threshold density must be used. Trial calculations showed that a combined observational sample of superclusters can be formed using the 2dFGRS sample with threshold density 6.0, and the SDSS DR4 sample with a thresh-

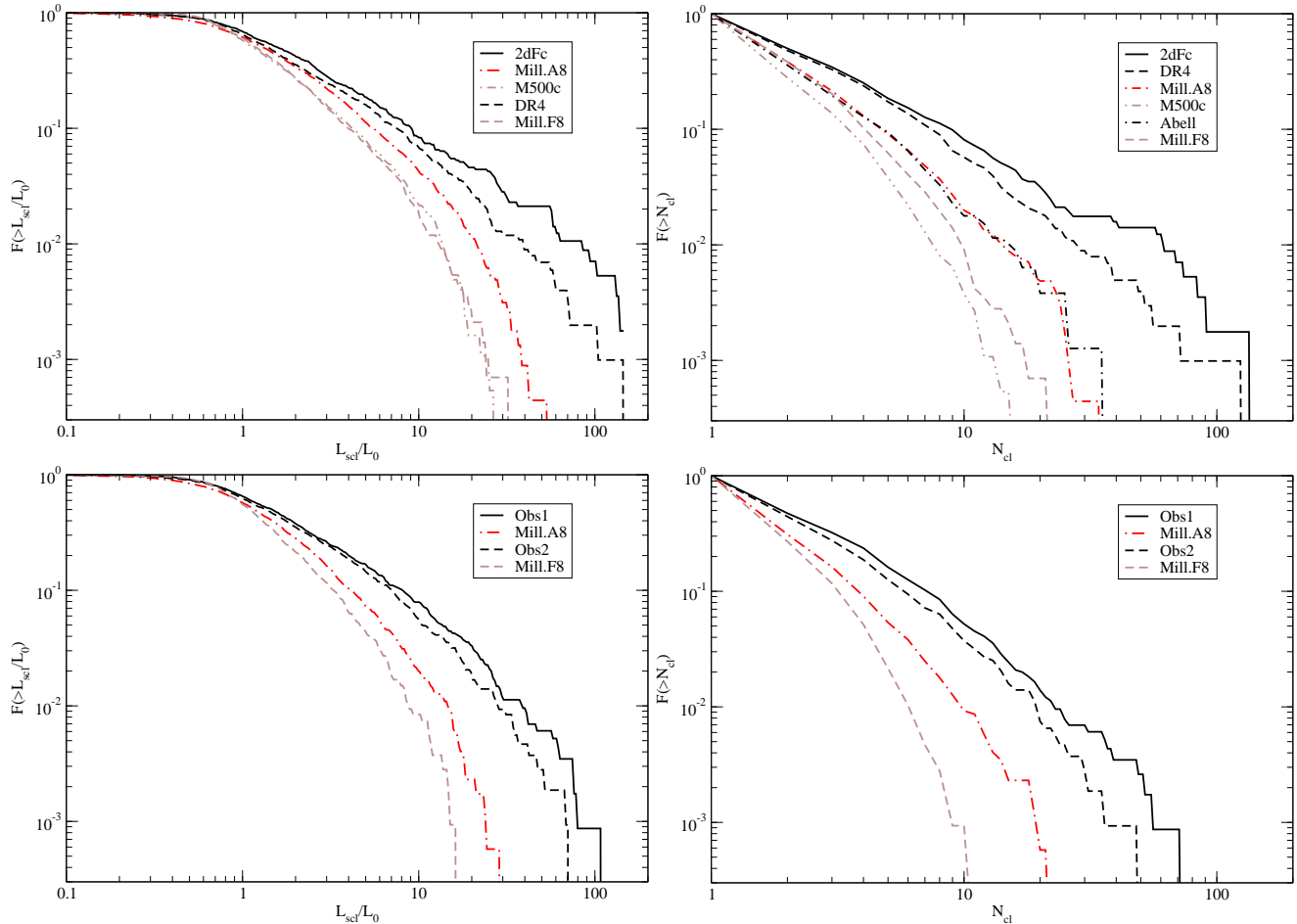


**Fig. 3.** Upper panels show the relative integrated luminosity/mass functions (left), and the multiplicity functions (right) of all real and simulated superclusters, found using threshold density 5.0. Luminosities/masses are expressed in units of mean luminosities/masses of superclusters of multiplicity 1,  $L_0$ , given in Table 1. Different lines mark supercluster samples: the 2dFGRS, the Sloan Digital Sky Survey DR4, the Millennium simulation full sample Mill.A8 and selected sample Mill.F8, the M500 sample and the sample of Abell superclusters. Lower panels show the comparison of the combined observational samples Obs1 and Obs2 with the Millennium simulation samples Mill.A8 and Mill.F8, using threshold density 6.0.

old density 5.0. To avoid the inclusion to the combined observational sample data of lower accuracy we used only superclusters of the main sample with distances up to  $520 h^{-1}$  Mpc. This combined sample Obs1 contains 1151 superclusters, 592 of them contain only 1 DF-cluster and were used in the calibration of relative luminosities of superclusters (for this sample we get  $L_0 = 6.73e+11$ ). The other combined observational sample Obs2 was found using threshold density 6.0 and distance limit  $520 h^{-1}$  Mpc in all subsamples.

The most striking feature of the Figure is the demonstration of the presence of numerous very luminous superclusters in observational samples, and the absence of such systems in simulated samples. This difference between real and simulated supercluster richness is well seen using both richness criteria, the multiplicity and luminosity functions. For threshold density 6.0 most luminous simulated superclusters have a relative luminosity of about 20 – 30 in terms of the mean luminosity of richness class 1 superclusters, most luminous superclusters of real samples have a relative luminosity about 100, i.e. they are about 3 times more luminous. The fraction of very luminous su-

perclusters (relative luminosity 20 and above) is about ten times higher in real samples than in simulated samples. Similar differences exist between the multiplicity functions of real and simulated supercluster samples. For threshold density 6.0 the richest model superclusters have a multiplicity of about 20 whereas real superclusters have over 50. The number of Abell clusters in the richest superclusters is about 30; this difference in the number of Abell and DF-clusters can be explained by differences in the number density of these cluster samples: the density of DF-clusters is about 2 times higher than that of Abell clusters. The differences between real and simulated samples are observed not only in the region of most luminous superclusters: over the whole richness scale the number of DF-clusters in simulated samples is smaller than in real superclusters.

One more interesting observation: very luminous superclusters are located in *all subsamples* (Northern and Southern regions of 2dFGRS, and in subregions of the SDSS DR4 sample, if divided into 3 wedges of equal width). These subsamples have characteristic volumes of about 10 million cubic  $h^{-1}$  Mpc, whereas model samples of 10 times larger volume have no

extremely rich superclusters. Kolmogorov-Smirnov test shows that the probability that real and model distributions of supercluster luminosities and richnesses are taken from the same parent distribution is  $10^{-10}$  and  $10^{-6}$ , respectively.

#### 4. Luminous superclusters and inflation

Superclusters of galaxies are formed by density perturbations of large scales. These perturbations evolve very slowly. As shown by Kofman & Shandarin (1988), the present structure on large scales is built-in already in the initial field of linear gravitational potential fluctuations. Actually they are remnants of the very early evolution and stem from the inflationary stage of the Universe (see Kofman et al. 1987). The distribution of luminosities (or masses) of superclusters allows us to probe processes acting at these very early phases of the evolution of the Universe.

One possible explanation for the large difference between the distribution of luminosities of real and simulated samples is the underestimate of the role of very large density perturbations. If this is the case then this means that our simulations have not yet reached a volume which can be treated as a fair sample of the Universe. In other words, a fair sample of the Universe has linear dimensions far in excess of  $500 h^{-1}$  Mpc, used in simulations investigated in this Letter. As shown by Power & Knebe (2006), variations in the box size in a smaller box do not influence properties of Dark Matter haloes in cosmological simulations.

The other feasible explanation of the differences between models and reality may be the presence of some unknown processes in the very early Universe which give rise to the formation of extremely luminous and massive superclusters.

To date it is too early to make definite conclusions on the character of processes during inflation which may have caused the formation of very massive superclusters. Some aspects of this problem were recently studied by Saar et al. (2006). They demonstrated that rich superclusters formed in places where large density waves combine in similar phases to generate high density peaks. The larger the wavelength of such phase synchronization, the higher the richness and mass of superclusters. The synchronization has properties of sound waves, where, in addition to the main frequency, overtones appear. In this context it is interesting to note that very rich superclusters have a tendency to form a quasi-regular network with characteristic scales 250 and  $120 h^{-1}$  Mpc, as demonstrated by Broadhurst et al. (1990) and Einasto et al. (1994, 1997b, 1997a).

The explanation of the physical origin of very massive superclusters is a challenge for theory. To get a more complete observational picture of the phenomenon, large contiguous deep redshift surveys are needed. Only contiguous surveys allow to detect very massive superclusters. This is one reason why the continuation of the SDSS survey is so important, until the whole Northern hemisphere is covered by redshift data, as originally planned.

*Acknowledgements.* We are pleased to thank the 2dFGRS and SDSS Teams for the publicly available data releases. The Millennium Simulation used in this paper was carried out by the Virgo

Supercomputing Consortium at the Computing Center of the Max-Planck Society in Garching. The present study was supported by Estonian Science Foundation grants No. 4695, 5347 and 6104 and 6106, and Estonian Ministry for Education and Science support by grant TO 0060058S98. This work has also been supported by the University of Valencia through a visiting professorship for Enn Saar and by the Spanish MCyT project AYA2003-08739-C02-01. J.E. thanks Astrophysikalisches Institut Potsdam (using DFG-grant 436 EST 17/2/05) and Uppsala Astronomical Observatory for hospitality where part of this study was performed. A.K. acknowledges funding through the Emmy Noether Programme by the DFG (KN 755/1). D.T. was supported by the US Department of Energy under contract No. DE-AC02-76CH03000.

#### References

- Abell, G., 1958, ApJS, 3, 211  
 Abell, G., 1961, AJ, 66, 607  
 Abell, G., Corwin, H., Olowin, R., 1989, ApJS, 70, 1  
 Adelman-McCarthy, J.K., Agüeros, M.A., Allam, S.S. et al. 2006, ApJS, 162, 38  
 Basilakos, S., 2003, MNRAS, 344, 602  
 Basilakos, S., Plionis, M., Rowan-Robinson, M., 2001, MNRAS, 323, 47  
 Broadhurst, T.J., Ellis, R.S., Koo, D.C. and Szalay, A.S., 1990, Nature, 343, 726  
 Colless, M.M., Dalton, G.B., Maddox, S.J., et al. , 2001, MNRAS, 328, 1039  
 Colless, M.M., Peterson, B.A., Jackson, C.A., et al. , 2003, (astro-ph/0306581)  
 Croton, D.J., Springel, V., White, S.D.M. et al. 2006, MNRAS, 365, 11  
 de Vaucouleurs, G., 1953, AJ, 58, 30  
 Einasto, J., Einasto, M., Gottlöber, S. et al. 1997a, Nature, 385, 139  
 Einasto, J., Einasto, M., Hütsi, G., et al. , 2003a, A&A, 410, 425 (E03a)  
 Einasto, J., Einasto, M., Saar, E. et al. 2006b, A&A, (submitted, Paper II, astro-ph/0604539 )  
 Einasto, J., Einasto, M., Tago, E. et al. 1999, ApJ, 519, 456  
 Einasto, J., Einasto, M., Tago, E. et al. 2006a, A&A, (submitted, Paper I, astro-ph/0603764)  
 Einasto, J., Einasto, M., Tago, E. et al. 2006c, (in preparation)  
 Einasto, J., Hütsi, G., Einasto, M., et al. , 2003b, A&A, 405, 425  
 Einasto, J., Tago E., Einasto, M., et al. 2005, A&A, 439, 45  
 Einasto, M., Einasto, J., Tago, E., Dalton, G. & Andernach, H., 1994, MNRAS, 269, 301 (E94)  
 Einasto, M., Einasto, J., Tago, E., Müller, V. & Andernach, H., 2001, AJ, 122, 2222  
 Einasto, M., Tago, E., Jaaniste, J., Einasto, J. & Andernach, H., 1997b, A&A Suppl., 123, 119  
 Erdogdu, P., Lahav, O., Zaroubi, S. et al. 2004, MNRAS, 352, 939  
 Fleenor, M.C., Rose, J.A., Christiansen, W.A. et al. 2005, AJ, 130, 957  
 Gao, L., White, S.D.M., Jenkins, A. et al. 2005, MNRAS, 363, 379  
 Gregory, S.A. & Thompson, L.A. 1978, ApJ, 222, 784  
 Jõeveer, M., Einasto, J. & Tago, E. 1978, MNRAS, 185, 357  
 Kalinkov, M. & Kuneva, I. 1995, A&A Suppl., 113, 451  
 Knebe, A., Green, A., Binney, J., 2001, MNRAS, 325, 845  
 Kofman, L.A., Linde, A.D. & Einasto, J. 1987, Nature, 326, 48  
 Kofman, L.A. & Shandarin, S.F. 1988, Nature, 334, 129  
 Nichol, R.C., Sheth, R.K., Suto, Y., et al. 2006, MNRAS, 368, astro-ph/0602548  
 Porter, S.C. & Raychaudhury, S. 2005, MNRAS, 364, 1387  
 Power, C. & Knebe, A. 2006, MNRAS (in press), astro-ph/0512281

- Proust, D., Quintana, H., Carrasco, E.R. et al. 2006, A&A, 447, 133  
Ragone, C.J., Muriel, H., Proust, D. et al. 2006, A&A, 445, 819  
Saar, E., Einasto, J., Einasto, M. et al. 2006, (in preparation)  
Springel, V., White, S.D.M., Jenkins, A. et al. 2005, Nature, 435, 629  
Tago, E., Einasto, J., Saar, E. et al. 2006a, AN, 327, 365 (T06)  
Tago, E., Einasto, J., Saar, E. et al. 2006b, (in preparation)  
Zeldovich, Ya.B., Einasto, J., Shandarin, S.F., 1982, Nature, 300, 407  
Zucca, E. et al. 1993, ApJ, 407, 470